

Research Article

Evaluation of the Osteoblast Behavior to PGA Textile Functionalized with RGD as a Scaffold for Bone Regeneration

Mariné Ortiz,¹ Diana María Escobar-García,¹ Marco Antonio Álvarez-Pérez,² Amaury Pozos-Guillén,¹ Christian Grandfils,³ and Héctor Flores¹

¹Basic Sciences Laboratory, Faculty of Stomatology, San Luis Potosí University, San Luis Potosí, SLP, Mexico

²Tissue Bioengineering Laboratory, Postgraduate and Research Division Studies, Faculty of Dentistry, National University of Mexico, Mexico City, Mexico

³Interfaculty Research Center of Biomaterials, Institute of Chemistry, University of Liège, Liège, Belgium

Correspondence should be addressed to Héctor Flores; heflores@uaslp.mx

Received 25 May 2017; Revised 9 October 2017; Accepted 23 October 2017; Published 20 November 2017

Academic Editor: Samuel M. Mugo

Copyright © 2017 Mariné Ortiz et al. This is an open access article distributed under the Creative Commons Attribution License, which permits unrestricted use, distribution, and reproduction in any medium, provided the original work is properly cited.

The new era of biomaterials for repairing bone tissue injury continues to be a challenge in bone tissue engineering. The fiber scaffolds allow for cellular interconnection and a microenvironment close to the bone extracellular matrix. The aim of this study was to evaluate the osteoblast behavior on a 3D textile of PGA (polyglycolic acid) fibers functionalized with the RGD (R: arginine; G: glycine; D: aspartic acid) peptide. The cell morphology, proliferation, and calcium phosphate deposition ability were evaluated on textiles at different time intervals under a confocal laser scanning microscope. The osteoblast viability ranged from 92% to 98%, and cell proliferation was higher in PGA-RGD than control PGA (uncoated). In addition, the osteoblast calcium phosphate deposition was significantly greater on PGA-RGD in osteogenic inductor medium (OIM) in contrast to controls without inducing factors. The PGA-RGD fibers supported proliferation and viability of osteoblast and stimulated bone osteogenesis and mineralization. These results support the adoption of this 3D polymeric textile as a scaffold for bone tissue engineering.

1. Introduction

The healing of damaged or diseased bone is still a challenge issue for orthopedic surgeon and craniofacial surgeon. To overcome reduced bone formation and healing, many have turned to regenerative medicine. Usually, autogenous bone grafting is the first choice for bridging the bone defect. The advantages are free of immunogenic response and completely biocompatible since it comes from patient himself. The disadvantages are limited donor source, donor site morbidities, and variable bone graft survival. Xenograft and allograft are alternative choices for the treatment. However, immunogenic reaction and inadequate bone regeneration due to incomplete resorption result in nonunion or pathologic fracture. Recently tissue engineering becomes a promising matter to improve bone defect reparation [1–4].

The tissue engineering approach is a promising strategy added in the field of bone regenerative medicine, which aims

to generate new, cell-driven, functional tissues, rather than just to implant nonliving scaffolds. The manufacture of scaffolds mimicking the extracellular bone matrix, which is composed of collagen fibers, calcium, phosphorus, and other minerals, has not yet been resolved [5–7]. Scaffolds made from polymer fibers have many of the characteristics necessary for the adhesion, proliferation, and differentiation of mesenchymal stem cells and osteoblasts [8–11]. Cell behavior can be influenced by the topography of fiber scaffolds; the organization, alignment, and direction of the fibers allow cells to attach to multiple textile walls due to their close interconnectivity and larger surface-area [12–15].

One of the goals of bone tissue engineering is to reproduce the biological and physiological conditions of bone within the human body by mimicking the *in vivo* cellular microenvironment, which consists of multiple complex factors. The ideal scaffold for bone engineering should promote mineralization and support the new osteoid matrix to do

this; biomaterial surfaces are modified and functionalized with bioactive factors that stimulate and promote a cellular response [16].

To repair bone defects and regenerate bone, the induction of osteogenesis is key. It is also a key determining the capacity of osteoblasts to deposit extracellular matrix and bone mineralization. The new biomaterials replace not only the mechanical functions but also the biological characteristics of the bone tissue [12, 17, 18].

Previous work demonstrated that the biocompatibility of a 3D polymeric textile intended for use in tissue regeneration was tested by evaluating the viability, proliferation, and adhesion of dental pulp stem cells (DPSCs); morphological parameters were characterized using scanning electronic microscopy (SEM), X-ray photoelectron spectroscopy (XPS), and X-ray microtomography (μ CT) analyses. The textiles were functionalized with the RGD (R: arginine; G: glycine; D: aspartic acid) peptide, which is thought to be the principal peptide responsible for cell adhesion [19]. Because synthetic polymers do not have bioactive groups on their surfaces, they do not promote cellular adhesion and require surface functionalization [20]. The 3D polymeric textile has been shown to support cell viability; however, it is necessary to perform studies with cell lineages specific to the tissue that needs to be regenerated [19].

In this study the behavior of osteoblast on PGA 3D textile functionalized with RGD to determine their ability induced of calcium phosphate deposition by used as scaffold for bone regeneration was evaluated. Additionally, the capacity of the scaffolds to induce osteoid matrix synthesis followed directly by mineralization was examined. The proliferation of osteoblasts on the fibers was evaluated by [3-(4,5-dimethylthiazol-2-yl)-5-(3-carboxymethoxyphenyl)-2-(4-sulfophenyl)-2H-tetrazolium] (MTS) assay, cell viability was evaluated with the LIVE/DEAD[®] Viability/Cytotoxicity Kit assay under a fluorescence microscope, and mineral deposition was evaluated with the Osteogenesis Quantitation Kit (Millipore).

2. Materials and Methods

2.1. Textile Fabrication and RGD Textile Functionalization. The textiles were fabricated and characterized as described in previous work. Briefly, the textiles were knitted by Centxebel (Verviers, Belgium) from resorbable thread made from polyglycolic acid (PGA) multifilaments. After cutting, cleaning, drying, and undergoing 2 hours of UV sterilization and generating textile samples of an overall dimension of $0.2 \times 0.5 \times 0.5$ cm (*h w d*), the materials were stored under vacuum at -20°C until future use. The RGD (R: arginine; G: glycine; D: aspartic acid, A8052 Sigma-Aldrich) was physically absorbed by the textiles by incubating them in a solution of RGD (1 mg/mL) plus 0.1 M PBS (phosphate saline buffer) for 6 h at 4°C . Next, the textiles were washed with PBS and dried for 1 h under sterile conditions. The μ CT and XPS analyses were conducted to analyze the porosity and surface properties of the fabrics, respectively [19].

2.2. Osteoblast Culture. Human osteoblasts (hOB) were isolated from the maxillary tuberosity using the explant technique during third molar surgery. This study was approved by

the Institutional Ethics Committee (UASLP CEIFE-032-012). The hOB was cultured in 75 cm^2 cell culture flasks containing Dulbecco's Modified Eagle Media (DMEM, Sigma-Aldrich, St. Louis, USA) supplemented with 10% fetal bovine serum (FBS, Biosciences, USA) and antibiotic solution (streptomycin 100 $\mu\text{g}/\text{mL}$ and penicillin 100 U/mL, Sigma-Aldrich). The cell cultures were incubated in a 100% humidified environment at 37°C in an environment of 95% O_2 and 5% CO_2 . The hOB from passages 2–6 were used for all of the experimental procedures. For *in vitro* osteogenic differentiation, cells were cultured in an osteogenic inductor medium (OIM) consisting of complete DMEM medium supplemented with 50 $\mu\text{g}/\text{mL}$ of ascorbic acid, 10 mM of b-Glycerophosphate, and 10^{-7} M of Dexamethasone (all from Sigma-Aldrich St. Louis, USA). During the experiment, the culture medium was changed twice per week.

2.3. Seeding on Textiles. The hOB were cultured in a 75 cm^2 cell culture flask upon reaching 90% confluence and then washed with PBS. The cell monolayer was detached using 1x Trypsin-EDTA (0.25%) solution (Gibco, Life Technologies, USA). The human osteoblastic cells were seeded at a concentration of 1×10^4 cells/textile onto the upper surface of the PGA textiles and allowed to infiltrate into the textiles within Millicell EZ SLIDE 8-well glass slides (Millipore-USA). The samples evaluated in the study were PGA-RGD and PGA with and without OIM induction. Cells were cultured without agitation at 37°C in a humidified atmosphere under 5% CO_2 . Conventional polystyrene 24-well culture plates were used as a control. The medium was changed twice per week [19].

2.4. Cell Viability. The cell viability was determined at 3, 9, and 12 days of cell culture with the *in vitro* LIVE/DEAD Viability/Cytotoxicity Kit assay (Invitrogen) according to manufacturer's instructions. The cells were observed under a confocal laser scanning microscope (CLSM, Leica Model DMI4000B, Germany) using a laser beam emitted at 488 nm and 532 nm wavelengths. Images were processed and analyzed using the LASAF[®] software (Leica, Germany). Adherent live and dead cells were counted manually based on 10 images (1×1 mm) per textile acquired randomly. The percent viability was calculated using the following formula: number of live cells/number of total cells at each time $\times 100$.

2.5. Cell Proliferation. Proliferation of hOB cells seeded onto PGA at a concentration of 1×10^4 cells/textile was quantified at 3, 5, and 7 days of culture using the Cell Titer 96TM Aqueous One Solution Cell Proliferation Assay (Promega), also known as the MTS assay. This assay is based on the ability of mitochondrial dehydrogenases in living cells to oxidize the MTS tetrazolium compound forming a colored formazan product that is soluble in tissue culture medium. The concentration of colored product is directly proportional to the number of metabolically active cells. The hOB seeded at the indicated times onto PGA textile material and PGA textile material functionalized with RGD were washed with PBS, incubated with fresh culture medium containing 20 μL of the stock solution, and incubated for 3 h at 37°C . After incubation, the absorbance was quantified by spectrophotometry at 490 nm

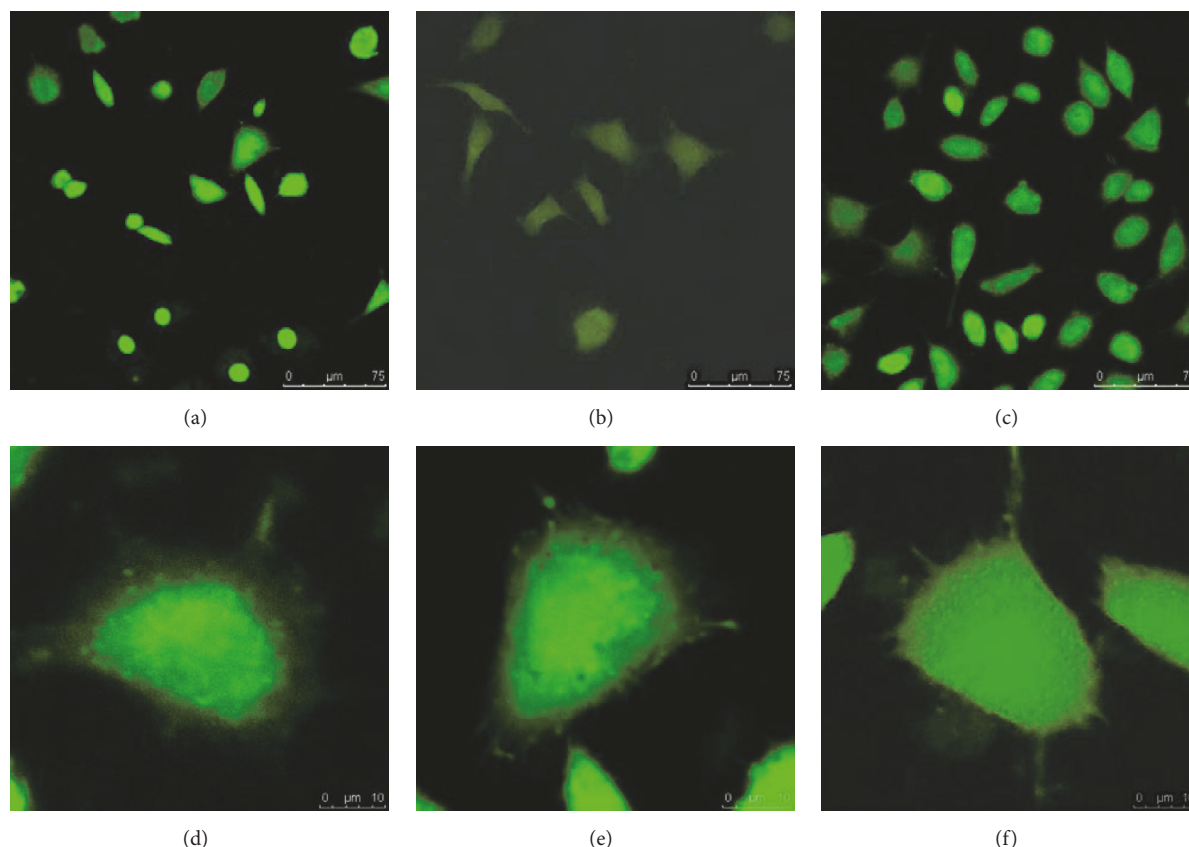


FIGURE 1: Image shows representative LIVE/DEAD fluorescent staining of osteoblasts seeded onto culture plates. 25% (a), 50% (b), and 75% (c) of osteoblasts showing flattened morphology at 3 days (d), 9 days (e), and 12 days (f).

with a plate reader (Epoch, BioTek). During the experiment, the culture medium was exchanged for fresh medium every two days. All MTS experiments were conducted in triplicate and repeated at least three times.

2.6. Mineralization Analysis and Calcium Phosphate Deposition. An osteogenesis quantization assay kit (Millipore) was used to determine the degree of mineralization, which is related to calcium content, during osteogenesis of human osteoblasts cultured onto the PGA textile for 4, 14, and 21 days with and without OIM. This assay is based on the quantification of Alizarin Red Stain (ARS), which binds selectively to calcium phosphate deposits (mineralization nodules). After incubation, the PGA textiles were carefully washed with PBS, fixed with 10% formaldehyde for 1 h at room temperature, carefully washed with distilled H₂O three times (5–10 minutes), and then stained with ARS solution (40 mM) for 30 min at room temperature. After several washes with distilled H₂O to remove excess dye, the PGA textiles were examined under an optical microscope (Leica DMIL LED), and images were processed and analyzed using the LAS EZ software (Leica, Germany). After microscopic analysis of ARS staining, the dye was extracted from the PGA textile by treatment with 10% acetic acid for 30 min. After neutralization with 10% ammonium hydroxide, the optical density of ARS was measured at 405 nm with a spectrophotometer

(Epoch, BioTek). The concentration of ARS was determined by correlating the absorbance of the experimental samples with a standard curve of known ARS dye concentrations.

2.7. Statistical Analysis. Significant differences between experimental groups were determined using the Kruskal-Wallis and Wilcoxon tests, with $p < 0.05$ considered significant. Data were analyzed using SigmaPlot Ver. 11.0 statistical software (SPSS Inc., Chicago, IL, USA).

3. Results

3.1. Cell Viability. The viability of human osteoblast cells isolated using the explant technique was evaluated by LIVE/DEAD Viability/Cytotoxicity Kit assay. The results show more than 92% viability with well-defined polygonal, spindle shaped cell morphology (Figures 1(a)–1(c)). The cell morphology was observed at different intervals throughout the viability assays (Figures 1(d)–1(f)). Our results showed that the viability of human osteoblasts cultured on PGA textile fibers functionalized with RGD peptide in the presence of OIM at 3, 9, and 12 days was significantly greater for all time intervals than viability of osteoblasts cultured on control PGA (Figures 2(a)–2(f)). However, no differences in biocompatibility were found when human osteoblasts were cultured onto PGA-RGD and PGA textile in normal complete medium

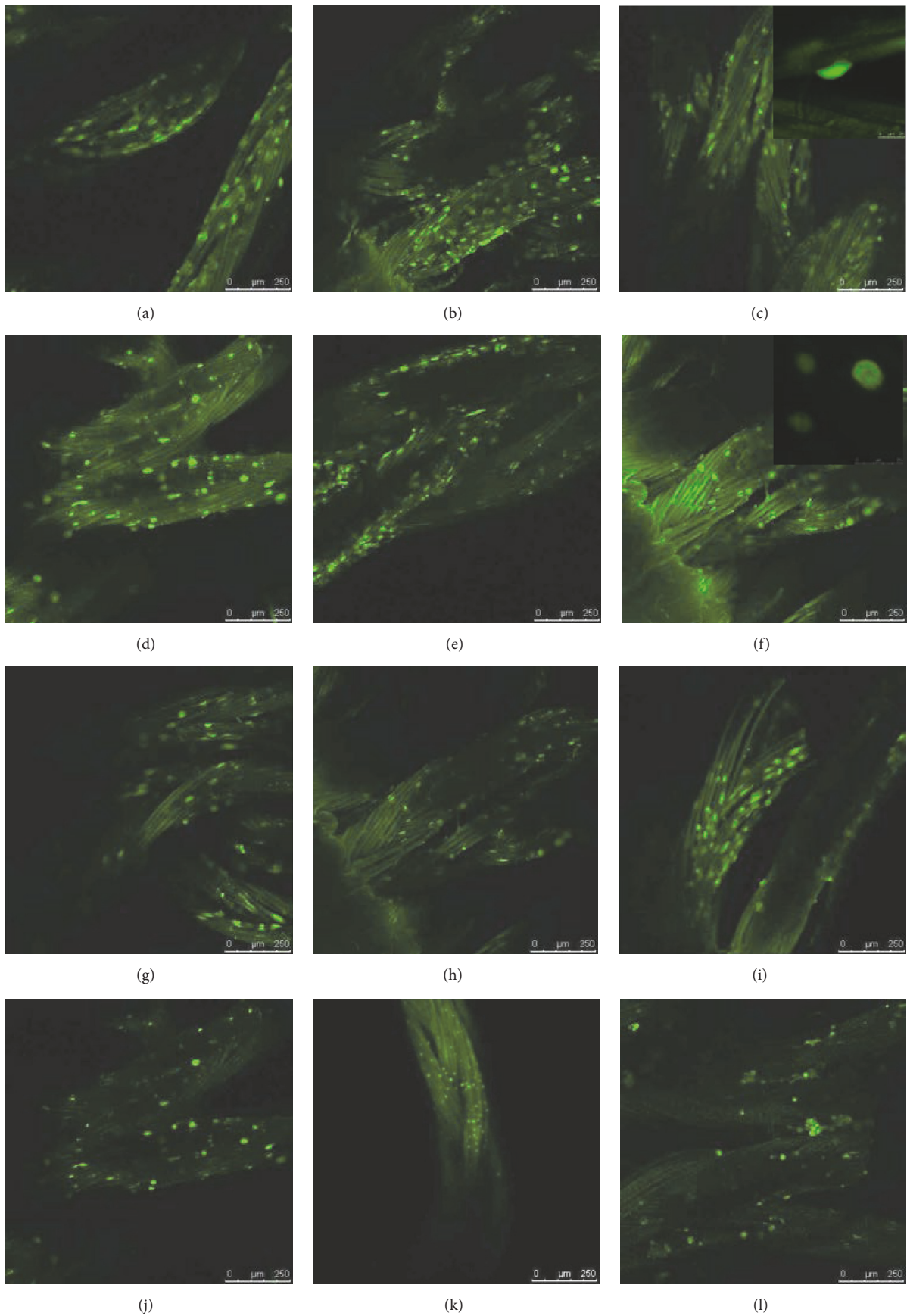


FIGURE 2: Images taken using a CLSM on PGA textiles at 3, 9, and 12 days. Osteoblasts were stained using the LIVE/DEAD Viability/Cytotoxicity Kit assay (10x). PGA-RGD-OIM at 3 days (a), 9 days (b), and 12 days (c). PGA-OIM at 3 days (d), 9 days (e), and 12 days (f). PGA-RGD control at 3 day (g), 9 days (h), and 12 days (i); control PGA at 3 days (j), 9 days (k), and 12 days (l).

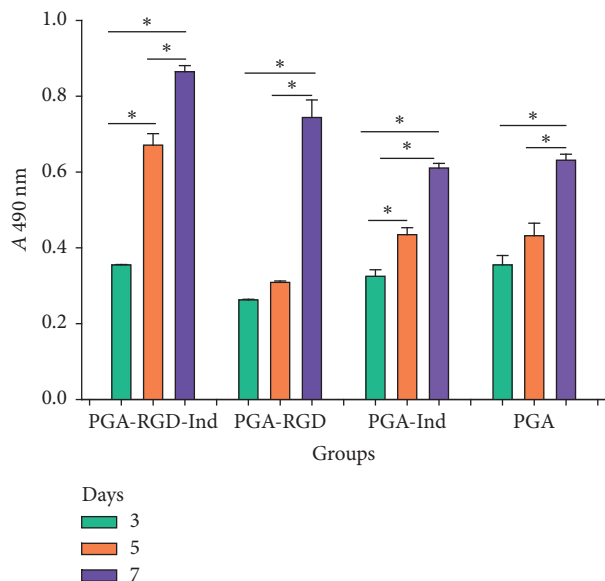


FIGURE 3: Osteoblast proliferation on the functionalized and non-functionalized textiles over time as measured by MTS assay, which represents active mitochondrial activity of living cells. Cell density was significantly higher on the PGA-RGD-OIM textile at 3, 5, and 7 days compared to control PGA * ($p < 0.05$). Cells proliferated faster on PGA-RGD than control PGA.

(Figures 2(g)–2(l)). The percent cell viabilities determined by image analysis of the PGA textiles ranged from 92% to 98%. Moreover, the morphology of human osteoblasts cultured on control PGA textiles were round to oval in shape compared to the flattened morphology of osteoblasts cultured on PGA-RGD (Figures 2(c) and 2(f)).

3.2. Cell Proliferation. Proliferation of osteoblasts cultured on both textile materials after 3, 5, and 7 days was evaluated using a proliferation assay kit. The absorbance level confirmed that human osteoblasts grow on PGA textiles in the presence and absence of OIM, indicating good proliferation without a cytotoxic response to the multifilament polymeric structures (Figure 3). The results showed that human osteoblasts grow faster on textiles of PGA functionalized with RGD peptide compared to the control PGA. Nevertheless, an increase in cell number was detected following growth on both surfaces during the course of the experiment. In the PGA-RGD-OIM group, there were significant differences between the three incubation times. The PGA-RGD only showed significant differences during the 3–7 day and 5–7 day intervals ($p < 0.05$). The PGA-OIM and PGA-RGD-OIM groups both showed significant differences at 3, 5, and 7 days. Comparing cell proliferation among the four groups at 3 days, there was a significant difference between PGA-RGD and control PGA. At 5 days, there were significant pairwise differences between all groups except PGA-OIM versus PGA. Lastly, at 7 days, there was also no significant difference for PGA-OIM versus PGA.

3.3. Mineralization Analysis and Calcium Phosphate Deposition. The amounts of calcium phosphate in the secreted

mineral matrix of osteoblasts were quantified using ARS. The osteoblasts cultured on both PGA-RGD and control PGA in the presence of OIM stained positive for the presence of mineral nodules of calcium by ARS staining assay at 4, 14, and 21 days. The results indicating that the mineral nodules increased in number and became larger with prolonged induction in OIM (Figures 4(a)–4(f)); in comparison with cells cultures on PGA-RGD and control PGA with complete normal medium, there was either a slight presence or absence of calcium phosphate deposits or mineral nodules (Figures 4(g)–4(l)). As a negative control, we used the osteoblasts cultured in plates with DMEM where calcium phosphate deposits did not form, and as a positive control, we used osteoblasts cultured in OIM.

Images of the mineral deposits were confirmed by quantitative analysis of ARS extraction, which indicated that polymeric textile scaffolds of PGA-RGD-OIM and control PGA-OIM have an enhanced calcium phosphate deposition in the extracellular matrix compared with cultures without OIM (Figure 5).

4. Discussion

Designing the ideal bone graft requires understanding the nature of the materials with which cells interact. Osteoinductive activity is one of the most important properties of the materials [21]. Methods exist to evaluate the behavior of cells on fibrous membrane surfaces tailored for bone tissue engineering [14]. In the present study, cell viability, proliferation, morphology, and calcium phosphate deposition by osteoblasts on the polymeric 3D textiles functionalized with RGD were evaluated.

The main characteristic of a biomaterial is its biocompatibility, and in our hands, the PGA-RGD fibers show a high level of cell viability (from 92% to 98%). This result could mean that the PGA-RGD fibers provide an appropriate environment for osteoblast cells where they can proliferate and migrate between multiple fibers and attach to the textile fibers and walls. In our previous studies, DPSCs were used and had a cell survival rate ranging from 94% to 100%. The parameters that probably play important roles in these textiles, such as surface roughness, 3D structure, and high interconnectivity, permit osteoblasts to migrate through the pores of the textiles and increase the surface available for protein adsorption, leading to cell attachment to the fibrous surface topographies of the PGA textile [19].

The morphology of the polymeric fiber textiles is a 3D structure with the fibers knitted in one orientation and aligned such that cells grow in the direction of the multifilaments. In previous studies that cultivated DPSCs on textiles, cells grew along the longitudinal axis of the fiber, which offers greater surface-area compared with monofilament mesh fabrics [19].

Studies have reported significantly higher cell mobility on aligned poly(methyl methacrylate) fibers than on random fibers, probably because there is less distance between the fibers and there is increased cell-cell communication [22]. Moreover, the cells orient, elongate, and spread along poly(styrene) fibers [16]. Alignment of cells is regulated by

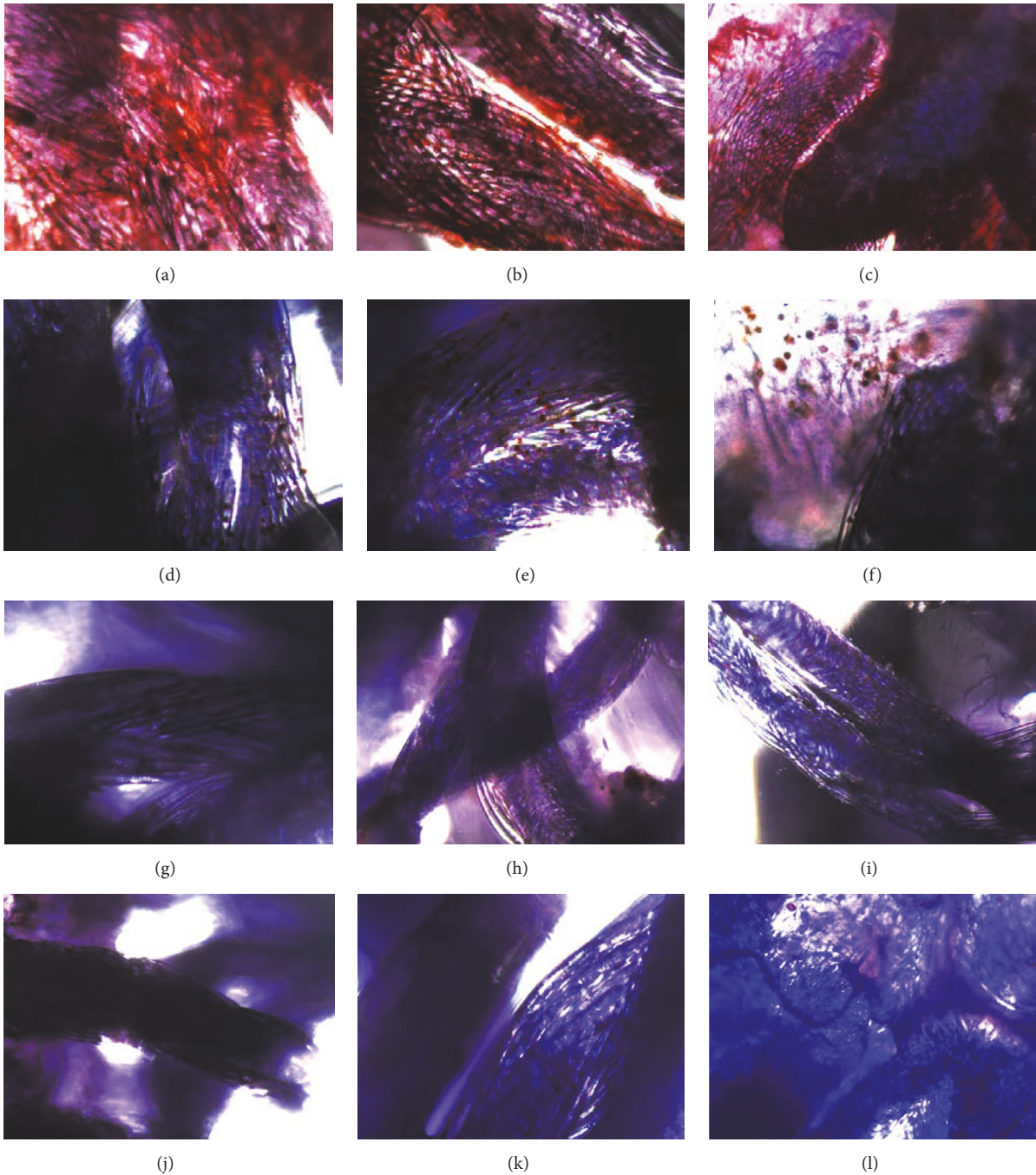


FIGURE 4: Cell aggregates grown in OIM stain positive with ARS solution, indicating osteoblast differentiation and mineralization. Phase contrast micrographs at a total magnification of 10x. PGA-RGD-OIM at 4 days (a), 14 days (b), and 21 days (c). PGA-OIM at 4 days (d), 14 days (e), and 21 days (f). In the case for the aggregates in non-OIM at 4, 14, and 21 days showed no calcium deposition; PGA-RGD at 4 days (g), 14 days (h), and 21 days (i). PGA at 4 days (j), 14 days (k), and 21 days (l).

fiber densities and patterns; therefore, the growth patterns depend on cell-cell communication and cell alignment [14].

The cell morphologies observed under CLSM include elongated and polygonal morphology and the presence of flattened and cytoplasmic extensions between the multifilaments. Cell infiltration is possible due to the porosity and the morphological parameters of the fiber. Cell morphology is one way to determine if the substrate is suitable for the cells.

The osteoblasts cultured on textiles had an elongated morphology with abundant cytoplasmic cell processes, filopodia, and lamellipodia, connected to the fiber matrix and to neighboring cells. These morphological characteristics are a key factor in many biological processes [23].

The proliferation assay demonstrated that all cells could proliferate after they adhered to the textiles. The fiber scaffold structures were shown to promote cell attachment;

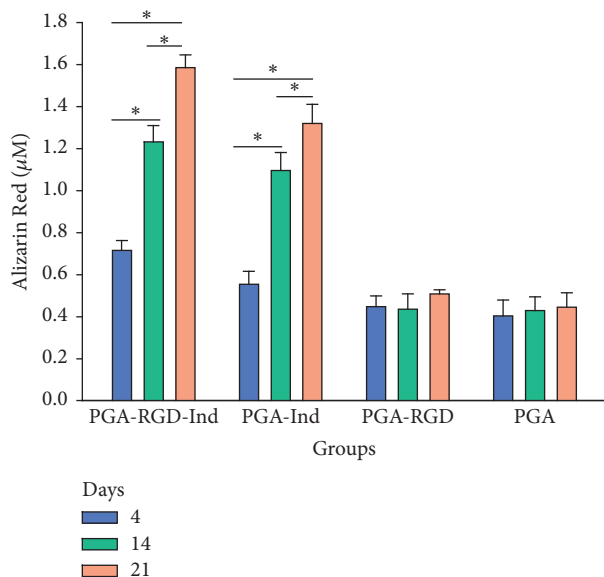


FIGURE 5: Quantitative Alizarin Red Staining after 4, 14, and 21 days of cell culture. There were significant differences on PGA-RGD and PGA with osteogenic inductor medium at 4, 14, and 21 days ($p < 0.05$).

nevertheless, surface functionalization stimulated protein adsorption, which represents the first step in cell adhesion. Studies have provided evidence that synthetic fibers may exhibit certain properties that are comparable to natural collagen fibers; thus, the nanofibrous architecture may be a superior scaffold versus the solid-walled architecture for promoting osteoblast differentiation and biomineralization [24–28].

Calcium phosphate deposition was evaluated by ARS staining, which is used to visually detect mineralization in bone tissue. In the textiles functionalized with RGD in the presence of OIM, the presence of ARS demonstrates calcium phosphate deposition throughout the multifilament polymeric textiles. In the case of control PGA without functionalization, but with osteoblasts cultured in OIM, lower amounts of ARS were observed. We supposed that RGD promotes the growth of osteoblasts and produces a greater amount of mineral nodules deposition on PGA-RGD. The growth rate of osteoblasts on control PGA textiles was slower than on functionalized textiles. This result may be related to the different degrees of cell spreading on these two surface types.

Studies have demonstrated that culturing osteoblast cells on nanofibers made of poly(L-lactic acid) results in much higher levels of alkaline phosphatase in cells than culturing on flat films in complete induction medium [29], while growth on polycaprolactone/gelatin electrospun scaffolds in medium with osteogenic supplementation promoted bone osteogenesis and mineralization [30]. In collagen/hydroxyapatite composite nanofibrous scaffolds, the mineralization reflects the functional activity of osteoblasts [31].

5. Conclusions

The interaction between osteoblasts and biomaterials depends on the biomaterial surface roughness, topography,

chemistry, and functionalization. The PGA textiles functionalized with RGD in inductive conditions tend to deposit calcium phosphate, which is an indicator of matrix formation. The osteoblast viability ranged from 92% to 98%, and cell proliferation was higher in PGA-RGD than control PGA. Our data showed that the adhesion and proliferation of osteoblasts cultured on PGA-RGD-OIM were significantly increased relative to control. In addition, the calcium phosphate deposition from osteoblasts was significantly greater on PGA-RGD-OIM. The PGA-RGD fibers supported proliferation and viability of osteoblast. These results suggest that this 3D polymeric textile can be employed as a scaffold for bone tissue regeneration. Future *in vivo* studies should be performed as well.

Conflicts of Interest

The authors declare that they have no conflicts of interest and any financial interest related to this study.

Acknowledgments

This work was partially supported by FNRS-CONACYT, Mexico-Belgium, Bilateral Collaboration “Biocompatibility of a New Polymeric Textile Proposed for Bone Tissue Regeneration,” Ref. V 4/285–NR/DeM–3.596, PIFI 2011-12, UASLP-C13-FAI-03-51.51, PFCE-UASLP 2016, PRODEP 2017, C15-FAI-10.78.78, and DGAPA-UNAM: PAPIIT-IN210815 Grants. Mariné Ortiz was a CONACYT Fellow 368667 and has received a grant from University of Liège, Belgium.

References

- [1] A. R. Amini, C. T. Laurencin, and S. P. Nukavarapu, “Bone tissue engineering: recent advances and challenges,” *Critical Reviews in Biomedical Engineering*, vol. 40, no. 5, pp. 363–408, 2012.
- [2] B. Schmidt-Rohlfing, C. Tzioupis, C. L. Menzel, and H. C. Pape, “Tissue engineering of bone tissue : PPPinciples and clinical applications,” *Der Unfallchirurg*, vol. 112, no. 9, pp. 785–795, 2009.
- [3] E. M. Younger and M. W. Chapman, “Morbidity at bone graft donor sites,” *Journal of Orthopaedic Trauma*, vol. 3, no. 3, pp. 192–195, 1989.
- [4] J. C. Banwart, M. A. Asher, and R. S. Hassanein, “Iliac crest bone graft harvest donor site morbidity: a statistical evaluation,” *The Spine Journal*, vol. 20, no. 9, pp. 1055–1060, 1995.
- [5] H. J. Park, K. D. Min, M. C. Lee et al., “Fabrication of 3D porous SF/ β -TCP hybrid scaffolds for bone tissue reconstruction,” *Journal of Biomedical Materials Research Part A*, vol. 104, no. 7, pp. 1779–1787, 2016.
- [6] H. J. Park, O. J. Lee, M. C. Lee et al., “Fabrication of 3D porous silk scaffolds by particulate (salt/sucrose) leaching for bone tissue reconstruction,” *International Journal of Biological Macromolecules*, vol. 78, pp. 215–223, 2015.
- [7] Z. Guo, J. Xu, S. Ding, H. Li, C. Zhou, and L. Li, “In vitro evaluation of random and aligned polycaprolactone/gelatin fibers via electrospinning for bone tissue engineering,” *Journal of Biomaterials Science, Polymer Edition*, vol. 26, no. 15, pp. 989–1001, 2015.

- [8] J. M. Holzwarth and P. X. Ma, "Biomimetic nanofibrous scaffolds for bone tissue engineering," *Biomaterials*, vol. 32, no. 36, pp. 9622–9629, 2011.
- [9] N. Wismer, S. Grad, G. Fortunato, S. J. Ferguson, M. Alini, and D. Eglin, "Biodegradable electrospun scaffolds for annulus fibrosus tissue engineering: Effect of scaffold structure and composition on annulus fibrosus cells in vitro," *Tissue Engineering Part: A*, vol. 20, no. 3–4, pp. 672–682, 2014.
- [10] W. Zhao, J. Li, K. Jin, W. Liu, X. Qiu, and C. Li, "Fabrication of functional PLGA-based electrospun scaffolds and their applications in biomedical engineering," *Materials Science & Engineering C: Materials for Biological Applications*, vol. 59, pp. 1181–1194, 2016.
- [11] H. Peng, Z. Yin, H. Liu et al., "Electrospun biomimetic scaffold of hydroxyapatite/chitosan supports enhanced osteogenic differentiation of mMSCs," *Nanotechnology*, vol. 23, no. 48, Article ID 485102, 2012.
- [12] W.-H. Lin, J. Yu, G. Chen, and W.-B. Tsai, "Fabrication of multi-biofunctional gelatin-based electrospun fibrous scaffolds for enhancement of osteogenesis of mesenchymal stem cells," *Colloids and Surfaces B: Biointerfaces*, vol. 138, pp. 26–31, 2016.
- [13] L. Terranova, R. Mallet, R. Perrot, and D. Chappard, "Polystyrene scaffolds based on microfibers as a bone substitute; development and in vitro study," *Acta Biomaterialia*, vol. 29, pp. 380–388, 2016.
- [14] J.-C. Chang, S. Fujita, H. Tonami, K. Kato, H. Iwata, and S.-H. Hsu, "Cell orientation and regulation of cell-cell communication in human mesenchymal stem cells on different patterns of electrospun fibers," *Biomedical Materials*, vol. 8, no. 5, Article ID 055002, 2013.
- [15] T. Schneider, B. Kohl, T. Sauter et al., "Influence of fiber orientation in electrospun polymer scaffolds on viability, adhesion and differentiation of articular chondrocytes," *Clinical Hemorheology and Microcirculation*, vol. 52, no. 2–4, pp. 325–336, 2012.
- [16] A. Serafim, R. Mallet, F. Pascaretti-Grizon, I.-C. Stancu, and D. Chappard, "Osteoblast-like cell behavior on porous scaffolds based on poly(styrene) fibers," *BioMed Research International*, vol. 2014, Article ID 609319, 2014.
- [17] M. Stoppato, H. Y. Stevens, E. Carletti, C. Migliaresi, A. Motta, and R. E. Guldborg, "Influence of scaffold properties on the inter-relationship between human bone marrow derived stromal cells and endothelial cells in pro-osteogenic conditions," *Acta Biomaterialia*, vol. 25, pp. 16–23, 2015.
- [18] M. Ngiam, L. T. Nguyen, S. Liao, C. K. Chan, and S. Ramakrishna, "Biomimetic nanostructured materials: potential regulators for osteogenesis?" *Annals Of the Academy of Medicine Singapore*, vol. 40, no. 5, pp. 213–222, 2011.
- [19] M. Ortiz, R. Rosales-Ibáñez, A. Pozos-Guillén et al., "DPSC colonization of functionalized 3D textiles," *Journal of Biomedical Materials Research Part B: Applied Biomaterials*, vol. 105, no. 4, pp. 785–794, 2017.
- [20] E. Ruoslahti, "RGD and other recognition sequences for integrins," *Annual Review of Cell and Developmental Biology*, vol. 12, pp. 697–715, 1996.
- [21] P. Janicki and G. Schmidmaier, "What should be the characteristics of the ideal bone graft substitute? Combining scaffolds with growth factors and/or stem cells," *Injury*, vol. 42, supplement 2, pp. S77–S81, 2011.
- [22] Y. Liu, A. Franco, L. Huang, D. Gersappe, R. A. F. Clark, and M. H. Rafailovich, "Control of cell migration in two and three dimensions using substrate morphology," *Experimental Cell Research*, vol. 315, no. 15, pp. 2544–2557, 2009.
- [23] E. Cukierman, R. Pankov, D. R. Stevens, and K. M. Yamada, "Taking cell-matrix adhesions to the third dimension," *Science*, vol. 294, no. 5547, pp. 1708–1712, 2001.
- [24] P. Jayakumar and L. Di Silvio, "Osteoblasts in bone tissue engineering," *Proceedings of the Institution of Mechanical Engineers, Part H: Journal of Engineering in Medicine*, vol. 224, no. 12, pp. 1415–1440, 2010.
- [25] J. M. Kanczler and R. O. Oreffo, "Osteogenesis and angiogenesis: the potential for engineering bone," *European Cells & Materials*, vol. 15, pp. 100–114, 2008.
- [26] K. M. Woo, J.-H. Jun, V. J. Chen et al., "Nano-fibrous scaffolding promotes osteoblast differentiation and biomineralization," *Biomaterials*, vol. 28, no. 2, pp. 335–343, 2007.
- [27] K. M. Woo, V. J. Chen, and P. X. Ma, "Nano-fibrous scaffolding architecture selectively enhances protein adsorption contributing to cell attachment," *Journal of Biomedical Materials Research. Part A*, vol. 67, no. 2, pp. 531–537, 2003.
- [28] M. P. Prabhakaran, J. Venugopal, and S. Ramakrishna, "Electrospun nanostructured scaffolds for bone tissue engineering," *Acta Biomaterialia*, vol. 5, no. 8, pp. 2884–2893, 2009.
- [29] J. Hu, X. Liu, and P. X. Ma, "Induction of osteoblast differentiation phenotype on poly(L-lactic acid) nanofibrous matrix," *Biomaterials*, vol. 29, no. 28, pp. 3815–3821, 2008.
- [30] M. A. Alvarez Perez, V. Guarino, V. Cirillo, and L. Ambrosio, "In vitro mineralization and bone osteogenesis in poly(ϵ -caprolactone)/gelatin nanofibers," *Journal of Biomedical Materials Research. Part A*, vol. 100, no. 11, pp. 3008–3019, 2012.
- [31] J. Venugopal, S. Low, A. T. Choon, T. S. S. Kumar, and S. Ramakrishna, "Mineralization of osteoblasts with electrospun collagen/hydroxyapatite nanofibers," *Journal of Materials Science: Materials in Medicine*, vol. 19, no. 5, pp. 2039–2046, 2008.



Hindawi

Submit your manuscripts at
<https://www.hindawi.com>

